

1 **Using scintillometry to assess reference evapotranspiration methods and their**
2 **impact on the water balance of olive groves**

3

4 Minacapilli M.¹, Cammalleri C.², Ciraolo G.³, Rallo G.⁴, Provenzano G.⁵

5

6 1) Department of Agricultural and Forest Sciences (SAF), Università degli Studi di Palermo, Viale
7 delle Scienze Ed. 4, 90128 Palermo, Italy. mario.minacapilli@unipa.it

8 2) European Commission, Joint Research Centre (JRC), via E. Fermi 2749, Bldg. 100, 21027
9 Ispra (VA), Italy. carmelo.cammalleri@jrc.ec.europa.eu

10 3) Department of Civil, Environmental, Aerospace, Materials Engineering (DICAM), Università
11 degli Studi di Palermo, Viale delle Scienze Ed. 8, 90128 Palermo, Italy.
12 giuseppe.ciraolo@unipa.it

13 4) Department of Agriculture, Food and Environment (DAFE), Università di Pisa, Via del
14 Borghetto 80, 56124 Pisa, Italy. giovanni.rallo@unipi.it

15 5) Department of Agricultural and Forest Sciences (SAF), Università degli Studi di Palermo, Viale
16 delle Scienze Ed. 4, 90128 Palermo, Italy. giuseppe.provenzano@unipa.it

17

18 **Corresponding author:** Mario Minacapilli. E-mail: mario.minacapilli@unipa.it

19

20 **Abstract**

21 Reference evapotranspiration (ET_0) is widely used for irrigation scheduling, to promote the
22 efficient use of water resources, the sustainability of agro-ecosystem productivity, as well as to
23 manage water quality and other environmental concerns. As suggested by ASCE-EWRI and FAO,
24 standard Penman-Monteith methods are generally applied for the accurate estimations of ET_0 , from
25 hourly to daily scale. In the absence of detailed meteorological information several simplified
26 equations, using a limited number of variables, have been alternatively proposed. In this paper, the
27 performance of different reference evapotranspiration methods, at hourly (Penman-Monteith,
28 Priestley-Taylor, Makkink and Turc) and daily scale (Penman-Monteith, Blaney and Criddle,
29 Hargreaves, Priestley-Taylor, Makkink and Turc), was initially evaluated based on scintillometer
30 measurements collected during six month, in 2005, in an experimental plot maintained under
31 “reference” conditions (alfalfa crop).

32 The daily values of ET_0 obtained with the examined methodologies were then used as input in
33 FAO-56 agro-hydrological model, in order to evaluate, for an olive grove in a Mediterranean
34 environment, the errors associated to simulated actual evapotranspiration.

35 Experiments were carried out in South West of Sicily, in an area where olive groves are the major
36 crop. The comparison between estimated and measured fluxes confirmed that FAO-56 Penman-
37 Monteith (PM) standardized equation is characterized by the lowest mean bias error (-0.15 mmd^{-1}
38 and 0.06 mmd^{-1} using daily or hourly data respectively)

39 However, the analysis also evidenced that the Priestley-Taylor equation can be considered a valid
40 alternative for the accurate estimation of ET_0 , characterized by a mean bias error of 0.35 mmd^{-1} and
41 0.43 mmd^{-1} using daily or hourly data respectively

42 The application of the FAO-56 water balance model, evidenced how, on the investigated olive
43 groves the best estimations of actual evapotranspiration are associated to the Priestley-Taylor ET_0
44 equation, confirming that the approach has to be considered a valid alternative to Penman-
45 Monteith ET_0 .

46

47 **Key-words:** Scintillometer; Evapotranspiration; Mediterranean climate; Micrometeorology.

48

49

50 **Introduction**

51 Evapotranspiration (ET) is one of the most important components of the hydrological cycle, and
52 its modelling is crucial for a wide range of applications, including water resource management in
53 agriculture.

54 Among the factors affecting ET processes, the atmospheric forcing plays a fundamental role since
55 it characterizes the upper boundary layer. Commonly, ET is estimated by separating the effects of
56 meteorological conditions from the nature of crop surface and the soil water availability
57 (Doorenbos and Pruitt, 1977). For this reason, the concept of reference evapotranspiration, ET_0 ,
58 has been introduced to represent the atmospheric water demand, regardless of crop type, when
59 water availability is not a limiting factor (Allen et al. 1998).

60 Between the various standard reference surfaces (i.e., grass, alfalfa and pan), the Environmental
61 and Water Resources Institute of American Society of Civil Engineering (ASCE-EWRI) proposed
62 to refer to a short crop similar to clipped and cool-season grass or to a tall crop similar to full-cover
63 alfalfa (ASCE-EWRI, 2005).

64 A number of methods have been proposed to estimate ET_0 , which can be schematically divided in
65 the following categories: (1) combined energy-mass balance methods (e.g., Penman 1948,
66 Monteith 1965); (2) radiation-based methods (e.g., Priestley and Taylor 1972); (3) temperature-
67 based methods (e.g., Blaney and Criddle, 1950); (4) mass transfer-based methods (e.g. Trabert,
68 1896, WMO, 1966, Mahringer, 1970); (5) pan evaporation-based models (Liu et al., 2004). The
69 distinction of these methodologies is generally based on the number of atmospheric variables used
70 as input, like air temperature, wind speed, air relative humidity and solar or net radiation.
71 Commonly, the Penman-Monteith (PM) equation has been adopted as standard method to estimate
72 ET_0 , because it combines the energy and mass balances and accounts for the fundamental physical
73 principles. Due to its incorporation of the physical processes, the Food and Agriculture
74 Organization, FAO (Allen et al. 1998) and later on also the ASCE-EWRI (ASCE-EWRI, 2005)
75 detailed the procedures to compute ET_0 according to the PM equation. However, although these
76 procedures are very reliable, they need a number of meteorological variables (including wind
77 speed and air relative humidity) that may not be available or not at the required time step.
78 Therefore, several simplified semi-empirical methods requiring a lower number of climatic
79 variables have been proposed under different environmental conditions. These methods generally
80 use solar radiation and/or air temperature data only, and their applicability is usually limited to
81 climate conditions that are similar to those where they were developed (Jensen and Haise, 1963).

82 Several review's papers of these methods, including PM equation have been recently published
83 (Kumar et. al., 2012; Valipour and Eslamian, 2014; Valipour, 2015a,b). Among the radiation-
84 based methods, the Priestley and Taylor (1972) and the Makkink (1957) equations, have been
85 extensively and successfully used at hourly time step, even for remote sensing-based applications
86 aimed at ET_0 estimate (De Bruin et al., 2010; Cammalleri and Ciruolo, 2013; Valipour, 2015c,d,e).
87 Moreover, several studies have been carried out in order to propose comparisons between
88 simplified approaches and more robust methods, like the PM in its different formulations, usually
89 assumed as the reference (Todorovic et al., 2013; Valiantzas, 2013; Valipour, 2014a,b,c; Djaman
90 et al., 2015; Valipour, 2015f). Despite the PM equation being usually considered as a reliable
91 reference of the 'true' ET_0 , it should be noticed that only a limited number of papers have been
92 focusing on the comparisons between estimated and measured ET_0 , mainly due to the lack of
93 reliable in-situ measurements

94 When considering simplified formulations, it is imperative that such formulations should be
95 routinely tested with field observations.

96 Other concerns are related to the limited number of full weather stations in various regions of their
97 world as well as the location, sometimes not optimal.. It is well-known, in fact, that air temperature
98 and relative humidity measured on rather dry surfaces can differ significantly from well-watered
99 fields of the same area, leading to an overestimation of ET_0 due to unreliable estimations of actual
100 water vapor deficit. This is an additional reason why in the Mediterranean environments, the PM-
101 based ET_0 estimations obtained by using meteorological data from common weather stations, have
102 to be tested with field measurements.

103 The first objective of this study is to assess the performances of seven equations to estimate ET_0
104 at different time steps (i.e., hourly and daily), by contrasting the estimates against laser
105 scintillometer surface flux measurements collected over a well-watered alfalfa (*Medicago sativa*
106 L.) field characterized by semiarid climate and dry summer seasons. The considered methods
107 include the PM equation in the versions suggested by FAO 56 and ASCE-EWRI, as well as some
108 simplified approaches, such as the Priestley and Taylor (1972), the Makkink (1957), the Turc
109 (1961), the Blaney-Criddle (1950) and the Hargreaves-Samani (1985) relationships.

110 Secondly, the values of daily ET_0 obtained with the different methodologies were used as input in
111 the FAO 56 agro-hydrological model, in order to quantify the impacts of the different formulations
112 on the actual evapotranspiration simulated for an olive grove in a typical Mediterranean
113 environment.

114

115 **Theoretical background**

116 Two main crops have been traditionally considered as the reference crop, i.e. grass and alfalfa. The
117 former, referring to a type of grass similar, in terms of physiological and structural characteristics,
118 to perennial ryegrass (*Lolium perenne* L.) or tall fescue (*Festuca arundinacea* Schreb) has been
119 preferred by researchers. However, alfalfa has been also used to describe reference
120 evapotranspiration thanks to its similarity in terms of leaf area index, roughness and physical
121 characteristics to many other common agronomic crops . In order to ensure “standard conditions”,
122 whatever is the reference crop, it is necessary to apply suitable agronomic management practices
123 According to Allen et al. (1998), reference evapotranspiration (ET_0) is defined as “the rate of
124 evapotranspiration from a hypothetical reference crop with an assumed crop height of 0.12 m, a
125 fixed surface resistance of 70 sec m^{-1} and an albedo of 0.23, closely resembling the
126 evapotranspiration from an extensive surface of green grass of uniform height, actively growing,
127 well-watered, and completely shading the ground”.

128 Based on the model developed by Penman (1948), later adapted by Monteith (1965), reference
129 evapotranspiration, ET_0 (mm h^{-1}), can be expressed as:

$$130 \quad ET_0 = \frac{0.408\Delta(R_{n,sw} - R_{n,lw} - G_0) + \gamma \frac{C_n}{T_a} u_2 (e_s - e_a)}{\Delta + \gamma(1 + C_d u_2)} \quad (1)$$

131 where $R_{n,sw}$, $R_{n,lw}$ and G_0 ($\text{MJ m}^{-2} \text{h}^{-1}$) are the short-wave and long-wave net radiations and soil heat
132 flux, respectively, T_a (K) is the air temperature at 2 m height, u_2 (m s^{-1}) is the wind speed at 2 m
133 height, e_s and e_a (kPa) are the saturation and actual vapor pressure, respectively, Δ (kPa K^{-1}) is the
134 slope of vapor pressure curve, γ (kPa K^{-1}) is psychrometric constant and, finally, C_n and C_d are two
135 coefficients depending on the reference surface.

136 The standardized procedures proposed by FAO 56 (Allen et al. 1998) and ASCE-EWRI (2005)
137 use in both cases eq. 1, even if they differ in the way to quantify the soil heat flux and the
138 coefficients C_n and C_d . In this paper, ET_0 values computed by using the FAO 56 procedure were
139 named PM-FAO, whereas those computed with ASCE-EWRI method, for short canopy, were
140 defined as PM-ASCE

141 The short-wave net radiation, $R_{n,sw}$ ($\text{MJ m}^{-2} \text{h}^{-1}$), can be evaluated as:

$$142 \quad R_{n,sw} = (1 - \alpha)R_s \quad (2)$$

143 where R_s ($\text{MJ m}^{-2} \text{h}^{-1}$) is the incoming solar radiation and α is the surface albedo, assumed equal to
 144 0.23 for reference crop.

145 The long-wave net radiation, $R_{n, \text{lw}}$ ($\text{MJ m}^{-2} \text{h}^{-1}$), can be computed according to the formulation
 146 based on the Stefan-Boltzmann's law:

$$147 \quad R_{n, \text{lw}} = \sigma T_a^4 \left(0.34 - 0.14 \sqrt{e_a} \right) \left(1.35 \frac{R_s}{R_{s0}} - 0.35 \right) \quad (3)$$

148 where σ is the Stefan-Boltzmann constant ($2.04 \times 10^{-10} \text{ MJ m}^{-2} \text{ K}^{-4} \text{ h}^{-1}$) and R_{s0} ($\text{MJ m}^{-2} \text{h}^{-1}$) is the
 149 clear-sky solar radiation. The correction term for cloudiness (second factor in brackets) has to be
 150 constrained to assume always values higher than 0 ($R_s/R_{s0} > 0.26$).

151 The dependence of e_s , Δ and γ on T_a can be expressed according to the following relationships:

$$152 \quad e_s = 0.611 \exp \frac{17.27(T_a - 273)}{T_a - 35.7} \quad (4)$$

$$153 \quad \Delta = 4098 \frac{e_s}{(T_a - 35.7)^2} \quad (5)$$

$$154 \quad \gamma = 0.0675 \left(\frac{T_a - 0.0065q}{T_a} \right)^{5.256} \quad (6)$$

155 where q (m) is the elevation above the sea level. Additionally, once e_s is known, the actual vapor
 156 pressure, depending on the air relative humidity, RH (%), is:

$$157 \quad e_a = e_s \frac{\text{RH}}{100} \quad (7)$$

158 At daily time step soil heat flux G_0 was ignored because it is relatively small for a fully vegetated
 159 grass or alfalfa reference surface. On hourly time step, the magnitude of G_0 of a full covered grass
 160 surface can be computed as a fraction of R_n (sum of $R_{n, \text{sw}}$ and $R_{n, \text{lw}}$), whose value differs for night-
 161 hours ($R_n \leq 0$) and day-hours ($R_n > 0$) respectively. Particularly FAO 56 assumes G_0 equal to $0.04R_n$
 162 and $0.2R_n$ for night-hours and day-hours, respectively, whereas in ASCE-EWRI the two fractions
 163 of R_n were fixed equal to 0.1 for day-hours and 0.5 for night hours.

164 With reference to the dimensionless coefficients of eq. 1, both FAO 56 and ASCE-EWRI proposed
 165 a value of 37 for C_n regardless of the time, Regarding the parameter C_d a constant value of 0.34 is
 166 used by by FAO 56, whereas ASCE-EWRI use a nighttime value for C_d of 0.96 and a value of
 167 0.24 during the daytime. It is interesting to notice that the two procedures adopted the same value
 168 of C_n , but different values of C_d . The latter, as reported by FAO 56, is a consequence of the constant

169 surface resistance, that was assumed equal to 70 s m^{-1} during the whole day. On the contrary, in
 170 ASCE-EWRI the differences can be ascribed to the surface resistance, assumed equal to 30, and
 171 200 s m^{-1} for day-time and night-time respectively.

172 Priestley and Taylor (1972), P&T, proposed a simplification of PM model, valid for extensive wet
 173 surface under minimum advection, for which the effects of aerodynamic component can be
 174 considered negligible if compared to the radiation component. According to these Authors, ET_0
 175 can be estimated as:

$$176 \quad ET_{0-P\&T} = 1.26 \frac{\Delta}{\Delta + \gamma} \frac{(R_n - G_0)}{\lambda} \quad (8)$$

177 Several studies (Castellví et al., 2001; Pereira, 2004; Baldocchi and Xu, 2007) have highlighted
 178 how the coefficient of 1.26 initially proposed, could be different and vary from 1.08 and to more
 179 than 1.60 due to the advectivity of the environment (Villalobos et al., 2002).

180 The Makkink (1957) formulation, later on resumed by de Bruin (1987), aims to provide reliable
 181 estimations of ET_0 , by only using R_s and T_a observations. This method can be seen as a further
 182 simplification of the P&T equation, where R_n is replaced with R_s and the empirical coefficient is
 183 conveniently redefined. Following this approach, ET_0 can be estimated as:

$$184 \quad ET_{0-MAK} = 0.61 \frac{\Delta}{\Delta + \gamma} R_s \quad (9)$$

185 Turc (1961) proposed an empirical approach to estimate ET_0 which is commonly used under humid
 186 conditions.

$$187 \quad ET_{0-TURC} = a_T 0.013 \frac{(T_a)}{(T_a + 15)} \frac{(23.8856R_s + 50)}{\lambda} \quad (10)$$

188 Trajković and Stojnić (2007) found that the reliability of Turc method strongly depends on wind
 189 speed, with overestimation under low wind speeds and underestimation during windy periods.

190 All these methods can be applied at hourly or daily time steps. On the contrary, the approaches
 191 proposed by Blaney and Criddle (Allen and Pruitt, 1991) and Hargreaves-Samani (1985) can be
 192 used only at daily temporal scale.

193 According to Blaney-Criddle method, reference evapotranspiration is:

$$194 \quad ET_{0-B\&C} = a \frac{\Delta}{\Delta + \gamma} R_s - b \quad (11)$$

195 where R_s ($\text{MJ m}^{-2} \text{ d}^{-1}$) is the daily solar radiation, a and b are correction coefficients.

196 When solar radiation, relative humidity and/or wind data are not available, ET_0 can be computed
 197 by means of Hargreaves-Samani model:

$$198 \quad ET_{0-HAR} = 0.0023 \left(\frac{T_{\max} - T_{\min}}{2} + 17.8 \right) \sqrt{T_{\max} - T_{\min}} \frac{R_a}{2.45} \quad (12)$$

199 where T_{\max} ($^{\circ}\text{C}$) and T_{\min} ($^{\circ}\text{C}$) are maximum and minimum daily air temperature, and R_a (MJ m^{-2}
 200 d^{-1}) is the extra-terrestrial solar radiation.

201 It is interesting to notice how the different proposed methodologies require a diverse number of
 202 meteorological variables, decreasing when passing from PM-based to radiation-based to
 203 temperature-based equations, as summarized in Table 1.

204

205 **Table 1 here**

206

207 ET_0 estimations based on the mentioned models have been initially compared, using classical
 208 statistical descriptors, with scintillometer measurements collected over a standard crop surface
 209 (alfalfa).

210 Daily ET_0 values obtained with the different procedures, were finally used as input data in FAO
 211 56 agro-hydrological model (Allen et al., 1998), in order to evaluate the corresponding effects on
 212 actual ET estimated for an olive grove.

213 According to the dual crop coefficient approach, actual evapotranspiration, ET , can be evaluated
 214 as:

$$215 \quad ET = T + E = (K_{cb}K_s + K_e)ET_0 = K_{c,adj}ET_0 \quad (13)$$

216 where K_{cb} is the basal crop coefficient obtained when the soil surface is dry, but transpiration
 217 occurs at potential rate, K_s is a dimensionless stress coefficient dependent on soil water content,
 218 SWC , and K_e describes the evaporation component from wet soil, following rain or irrigation
 219 (Allen and Pereira, 2009).

220 The values of K_s can be computed as:

$$221 \quad K_s = \frac{TAW - D_i}{TAW - RAW} \quad \text{for } D_i > RAW \quad (14a)$$

$$222 \quad K_s = 1 \quad \text{for } D_i \leq RAW \quad (14b)$$

223 where TAW (mm) is the total available water, D_i (mm) is the amount of daily water depleted out
 224 from root zone during the i -th day, and RAW (mm) is the readily available water. The latter can be
 225 evaluated as a fraction, p , of TAW , being p evaluated as:

$$226 \quad p = p_{table} + 0.04(ET_0 - 5) \quad (15)$$

227 Values of p_{table} for different crops were suggested by Allen et al. (1998). For the investigated
 228 system, p_{table} was set equal to 0.55.

229 The evaporation coefficient, K_e , can be also derived following the methodology described in the
 230 original publication requiring, however, measurements of soil water contents in the topsoil.

231 In absence of water stress ($K_s=1$ and negligible soil evaporation), K_{adj} returns to the standard crop
 232 coefficient K_c , as defined in the “single” approach (Doorenbos and Pruitt, 1977; Allen et al., 1998).

233 Although values of K_c and K_{cb} for some crops can be found in the literature (Allen and Pereira,
 234 2009), the proper local estimation of these coefficients for the examined olive groves was
 235 performed based on direct measurements (Minacapilli et al., 2009; Cammalleri et al., 2013a). In
 236 particular, K_{cb} and K_s were obtained by simultaneous measurements of evapotranspiration, crop
 237 transpiration and soil water content. The stress coefficient K_s was computed by eq. (14), in which:

$$238 \quad D_i = 1000 * (SWC_{fc} - SWC_{r,i}) * Z_r \quad (16)$$

$$239 \quad TAW = 1000 * (SWC_{fc} - SWC_{wp}) * Z_r \quad (17)$$

240 where SWC_{fc} and SWC_{wp} are the soil field capacity and wilting point, whereas Z_r is the rooting
 241 depth.

242

243 **Materials and Methods**

244 *Description of the study area and experimental layout*

245 The research was carried out from May to August 2005, in a commercial farm located near the
 246 town of Castelvetro, Sicily (37°38'46" N, 12°51'10" W), characterized by an average elevation
 247 of about 120 m above sea level. By following the USDA classification, soil can be classified as
 248 silty clay loam with average clay, silt and sand contents of about 24, 16 and 60%, respectively
 249 (Cammalleri et al. 2013b).

250 Crops on the farm are those typical of the Mediterranean environment, including olive, grapes and
 251 citrus. Olives, generally planted with an average density of about 250 trees per hectare, represent
 252 the main orchard crop in the area.

253 Experiments were carried out over a field of alfalfa (*Medicago sativa* L.) during the stationary
254 phase of crop biological cycle, by monitoring all the components of the surface energy balance
255 with a scintillometer station.

256 The crop was sown in the first decade of March 2005, with a sowing rate of 20 kg ha⁻¹ and,
257 according to the agronomic guidelines for hay crops, it was periodically cut down (every 7-10
258 days) in order to maintain the canopy at a uniform height of approximately 12-15 cm.

259 The field was maintained under reference standard conditions (Allen et al., 1998). A sprinkler
260 irrigation system was used to ensure an adequate crop water availability, avoiding soil water deficit
261 conditions. In order to evaluate the crop water availability, the preliminary hydraulic
262 characterization of the soil was carried out with standard laboratory procedures on undisturbed soil
263 samples collected at different depths (0-100 cm).

264 The classical evaporation technique allowed determination of the soil water retention curve, that
265 was mathematically described according to the van Genuchten equation (van Genuchten, 1980).

266 Soil water retention curves were determined on twenty undisturbed soil samples, 0.08 m diameter
267 and 0.05 m height, collected along 1 m vertical soil profile. Hanging water column apparatus and
268 pressure plate apparatus (Burke et al., 1986), were used to evaluate soil water contents
269 corresponding to soil matric potential values ranging from -0.05 to -153 m. The van Genuchten
270 model (van Genuchten, 1980) was used to fit experimental data; the water retention curve
271 parameters were obtained by means of the retention code, RETC (van Genuchten et al., 1992).

272 The soil water contents dynamics were monitored every 10 cm, from the soil surface to 120 cm
273 depth, by using a Diviner 2000 Sentek FDR (Frequency Domain Reflectometry) probe, after the
274 preliminary calibration of the sensor (Provenzano et al., 2015; Rallo and Provenzano, 2015).
275 Measurements were carried out every week, as well as before and after each irrigation event.
276 Values of soil water contents (*SWC*) measured at the different depths were then averaged in order
277 to determine, for each measurement day, a single value representative of the soil layer from where
278 the root water uptake mainly occurs.

279 Irrigation was scheduled according to the average soil matric potential in the root zone indirectly
280 estimated based on the soil water retention curve and measured soil water contents. Matric
281 potentials were in particular maintained always higher than -80 kPa, to avoid crop water deficit
282 conditions during the whole investigated period (Homaei et al., 2002). In this way it was possible
283 to account for the precipitation of the period. Total irrigation depth provided during the
284 experiments was equal to 122 mm, distributed in two equal events provided on 9th and 15th August.

285 Standard meteorological variables were acquired hourly, by a weather station belonging to Sicilian
286 Agrometeorological Information Service (SIAS, <http://www.sias.regione.sicilia.it>). The area is
287 characterized by the typical Mediterranean climate, with moderate rainfall during autumn and
288 winter, and high air temperature with scarce precipitation in summer.

289 A displaced-beam laser scintillometer (DBLS) installed in the field provided observations aimed
290 at estimating the surface energy balance terms allowing the evaluation of sensible heat, H , net
291 radiation, R_n , and soil heat, G , fluxes. Similarly to many others micro-meteorological techniques
292 (i.e., bowen ratio, surface renewal), scintillometry provides observations of ET as the residual term
293 of the surface energy budget equation, as:

$$294 \quad ET = \frac{R_n - G_0 - H}{\lambda} \quad (18)$$

295 Respect to other systems such as lysimeters, the distinct advantage of scintillometry is the ability
296 to derive surface energy balance terms over a long transect scaling from some ten of meters to
297 several kilometers. A detailed description of the DBLS used in the investigation, as well as the
298 related theory has been reported in appendix A.

299

300 **Results**

301 Firstly, the results of soil hydraulic characterization were analyzed in order to determine the water
302 availability in alfalfa field. Fig. 1 shows the soil matric potentials as a function of soil water
303 contents obtained at the different depths. According to the limited differences observed with
304 depths, a single equation was used to fit the experimental data.

305

306

Figure 1 here

307 Soil water content at field capacity (soil matric potential of -33 kPa) was equal to $0.42 \text{ cm}^3 \text{ cm}^{-3}$,
308 whereas at matric potential of -80 kPa, corresponding to the threshold of SWC below which crop
309 water stress occurs (Homaee et al., 2002; Kirkham, 2014), the soil water content was $0.18 \text{ cm}^3 \text{ cm}^{-3}$.
310

311 In order to check that standard conditions in alfalfa field occurred during the period of
312 investigation, the temporal variability of soil water status was monitored, from the soil surface to
313 a depth of 120 cm, using a Frequency Domain Reflectometry (FDR) probe.

314 Fig. 2 shows the temporal dynamic of daily precipitation P and irrigation I , shortwave radiation,
315 R_s , average air temperature, T , vapor pressure deficit, VPD and crop evapotranspiration obtained
316 with the scintillometer. The temporal dynamic of soil water content along the investigated profile
317 (0-120 cm) is also shown in the lowest panel. Unfortunately, the scintillometric acquisitions were
318 not continuous due to various technical problems causing the malfunctioning of the instrument,
319 and were limited to a total of 22 complete days. However, it has to be highlighted that all the
320 variables were registered with a time step of 15 minutes, composed of more than 2200 records.

321

322

Figure 2 here

323

324 The analysis of the climatic variables (Short wave radiation, Air temperature and Vapor pressure
325 deficit) showed R_s values around $300 \text{ W m}^{-2} \text{ d}^{-1}$, with a slightly decreasing trend from May to
326 August. Occasional reductions of solar radiation occurred during cloudy days or rain events. On
327 the contrary, the trend of average daily temperatures and the corresponding VPD values slowly
328 increased over time.

329 Precipitation and irrigations events maintained the soil (on average along the whole depth) at
330 sufficiently wet conditions, to avoid limitations on crop transpiration.

331 This is demonstrated by the analysis of temporal evolution of SWC along the investigated soil
332 profile (Fig. 2 - panel d). In fact, the minimum SWC in the layer 25-75 cm ranged between 0.10
333 and $0.14 \text{ cm}^3 \text{ cm}^{-3}$ due to the higher active root density charactering the layer, in the layers 0-25
334 cm and 75-100 cm, soil water contents resulted around $0.25 \text{ cm}^3 \text{ cm}^{-3}$ over the whole period. This
335 was due to the negligible contributes of soil evaporation in the top layer and root water uptake in
336 the lower layer. However, in the period before the 9th of August when the first irrigation event
337 occurred, the average SWC along the vertical profile decreased from $0.24 \text{ cm}^3 \text{ cm}^{-3}$ to 0.18 cm^3
338 cm^{-3} , a range of values characterizing absence of water stress conditions.

339 Daily ET_0 obtained by means of scintillometer measurements ranged between 3.2 mm d^{-1} and 6.0
340 mm d^{-1} , as a consequence of the combined effects of climatic variables such as solar radiation,
341 vapor pressure deficit and, only marginally, wind speed (data not shown).

342 At the begin of the experiment (around mid of May), despite the optimal water availability in the
343 soil (around $0.24 \text{ m}^3 \text{ m}^{-3}$), the observed values of ET_0 were not very high and around 4 mm d^{-1} ;
344 this fact can be explained by the relatively low VPD and air temperatures (low atmospheric
345 demand). From the end of May to the end of June, ET_0 increased to 5.5 mm d^{-1} thus showing that

346 the alfalfa was fully developed in a soil characterized by an average water content of about 0.21
347 $\text{m}^3 \text{m}^{-3}$, and responding to the atmospheric demand. In July, slight reductions of ET_0 values were
348 observed, as a consequence of the progressive decline of water availability along the soil profile,
349 in which SWC reached the threshold value of about $0.18 \text{m}^3 \text{m}^{-3}$ (first week of August). During the
350 second decade of August, despite the two irrigations events contributing to increase water
351 availability in the root zone, only a slightly increase of ET_0 was observed. This circumstance can
352 be explained by the contemporary reduction of the forcing factors (VPD , T and R_s).

353 For each reference evapotranspiration equation, Fig. 3 illustrates the cross comparison between
354 measured and estimated ET_0 at a daily time step. As can be observed, all the investigated equations
355 showed a certain dispersion around the 1:1 line, the highest accuracy in terms of determination
356 coefficient, R^2 , and root mean squares difference, (RMSD) was associated with the two methods
357 based on PM equation. These two approaches, applied at daily time step, gave practically identical
358 values, as shown in Fig. 3a. The negative R^2 values, observed when HAR and TURC methods are
359 applied, are a consequence of setting equal to zero the intercept of the considered regression
360 (estimated vs measured ET_0).

361

362

Figure 3 here

363

364 Because a statistical analysis based only on R^2 and RMSD can be misleading, a more exhaustive
365 comparison between measured and estimated daily ET_0 values was carried out according to the
366 Mean Absolute Difference (MAD), Slope of the regression equation, Relative Error (RE), Mean
367 Bias Error (MBE), and the scores, (T), obtained using the statistical T-test, whose values are
368 specified in Table 2.

369 These statistical descriptors confirmed the highest accuracy of PM methods also in terms of MAD,
370 Slope of the regression equation, RE, MBE and T. However, the P&T and MAK equation are
371 characterized by higher R^2 , but slopes of regression equation different from 1.0 which suggests
372 some bias that could be removed by a site-specific calibration procedure.

373

374

Table 2 here

375

376 A similar comparison was carried out at hourly time step and at daily scale obtained by aggregating
377 the resulting hourly ET_0 values.. Of course, in these comparisons the B&C and HAR equations
378 were not examined, because their application was originally proposed only for a daily time step.
379 Fig. 4 shows the comparisons between measured and estimated ET_0 at hourly time-step, whose
380 related statistical indicators are summarized in table 3 (hourly data). As can be observed from the
381 analysis of statistical indices a better performance can be associated with the PM-FAO56 equation.
382 However, comparing daily and hourly simulations the use of an hourly time step instead of daily
383 did not improve the performances of tested. In fact the higher values of R^2 obtained by the
384 statistical comparison (see Table 3) can be only ascribe to the higher magnitude values and data-
385 population of measured and estimated ET_0 values at hourly scale.

386

387

Figure 4 here

388

Table 3 here

389 Finally, daily ET_0 values obtained by the different equations, were used as input in FAO-56 agro-
390 hydrological model in order to assess the impact that the different equations have on actual
391 evapotranspiration estimated for an olive grove (ET).

392 ET values estimated by considering $ET_{0-PM-FAO}$ as input, were assumed as the benchmark,
393 accounting for the results of a previous model validation carried out in the same soil-plant-
394 atmosphere system (Rallo et al., 2012; Rallo et al., 2014).

395 Fig. 5a (upper panels) shows the results of the water balance simulations. As can be observed, all
396 the different ET_0 methods seem to reproduce similar patterns of simulated actual
397 evapotranspiration with differences mainly observed in the peaks. Since the FAO-56 agro-
398 hydrological model is a widely used tool to schedule irrigation on the base of simulated soil water
399 contents, the latter were also compared using all the different ET_0 methods. As can be observed in
400 Fig. 5b (lower panels) a significant variability was recognized in terms of soil water content that
401 certainly affect the scheduling of irrigations. In fact, assuming as time threshold value for
402 scheduling irrigation a soil water content value of $0.2 \text{ m}^3\text{m}^{-3}$ some differences can be realized
403 comparing the various scenarios plotted in Fig.5b. Particularly, using as input ET_0 values obtained
404 using PM, P&T and MAK equations, similar patterns of soil water content were obtained with a
405 resulting first irrigation identified around the end of the first decade of June. Differently, using
406 TURC, HAR and B&C equations for ET_0 estimation, the first irrigation should be applied at the
407 begin of June. Also in terms of number of scheduled irrigations the scenarios that can be deduced

408 analyzing the trends of Fig. 5b appear sometimes more different, as for the B&C case which seems
409 to suggest four date for irrigations instead of two.

410

411

412

Figure 5 here

413 **Final discussion and conclusions**

414 In the research, the performance of different methods to estimate ET_0 was tested in a typical
415 Mediterranean environment during spring-summer 2005, based on the comparison with
416 scintillometric measurements carried out on alfalfa reference crop. The need for this kind of
417 investigation arises from the consideration that in semi-arid environments, full weather datasets
418 required by PM based equations are often lacking, so that alternative and simplified approaches
419 characterized by a limited number of input variables, are required.

420 Experiments confirmed that PM-FAO56 formulation represents the best approach to estimate ET_0
421 at both hourly and daily time steps. Moreover, in the examined environment, when full weather
422 datasets are not available, satisfactory estimations of daily ET_0 can be obtained by using P&T and
423 MAK equations. The latter can be improved after a site-specific calibration.

424 The results suggested that: i) no systematic overestimations of ET_0 were caused by the suboptimal
425 location of standard weather station used to acquire the data; ii) the aerodynamic terms caused
426 slight differences between observed and estimated ET_0 obtained with the different methods,
427 whereas solar radiation had the major effects in the process. These considerations allows
428 confirmation that PM-based methods are able to reproduce fairly well evapotranspiration processes
429 in the investigated area and under the examined conditions. However, the small discrepancy
430 observed between measured and estimated ET_0 (PM-methods) can be ascribed to possible
431 differences between theoretical and actual reference surface conditions, as well as to presumable
432 measurement errors and of course not to the failure of the theoretical approach. For similar regions
433 in terms of climate, landscape and dominant crops, the P&T and MAK equations can be considered
434 reliable alternatives to the PM-based approaches, after site-specific parameter optimization when
435 a full weather dataset is not available,.

436 To assess the different approaches to estimate ET_0 , a functional evaluation was carried out by
437 using FAO-56 agro-hydrological model with input ET_0 values obtained from all the methods

438 evaluated here. The simpler P&T equation gave the best estimation of actual evapotranspiration,
439 confirming again that this method is a valid alternative to the PM-FAO56 method.
440 Finally, the use of scintillometry for validation purpose allowed the acquisition of reliable
441 observations at hourly (or shorter) time step, as well as to field-average data that are only slightly
442 affected by heterogeneity caused by field management practices.

443

444 **Acknowledgments**

445 The research was financed from Università degli Studi di Palermo (FFR 2012) and Ministero
446 dell'Istruzione, dell'Università e della Ricerca (PRIN 2010-2011), coordinated by G. Provenzano.
447 The contribution to the manuscript has to be shared uniformly among the authors. Special thanks
448 go to the Italian National Agency for New Technologies, Energy and Sustainable Economic
449 Development (ENEA) to provide the laser scintillometer (DBLS) installed in the field.

450

451 **APPENDIX A**

452 *Scintillometer measurements of evapotranspiration*

453 Scintillometry provides estimations of ET as residual term of the surface energy balance equation,
454 as:

$$455 \quad ET = \frac{R_n - G_0 - H}{\lambda} \quad (A1)$$

456 where H ($\text{MJ m}^{-2} \text{h}^{-1}$) is the sensible heat flux observed by the scintillometer and λ is the latent
457 heat of vaporization ($\approx 2.45 \text{ MJ kg}^{-1}$), whereas R_n and G_0 can be measured with common
458 instruments, i.e. net radiometers and flux plates.

459 Scintillometry retrieves H on the base of the optical distortion of a light beam caused by turbulence
460 in the atmosphere. DBLS measures the scintillations over two close parallel path beams produced
461 by a transmitter at the wavelength, λ_s , of 670 nm, and recorded by a receiver placed at a certain
462 distance, R (m).

463 The theory of DBLS can be found in Thiermann and Grassl (1992) which demonstrated that the
464 covariance of the logarithm of the amplitude of the received radiation is given by:

465
$$B_{12} = 0.124 C_n^2 K^{7/6} R^{11/6} f_B \left(\frac{l_0}{\sqrt{\lambda_s R}}, \frac{d_i}{\sqrt{\lambda_s R}}, \frac{D}{\sqrt{\lambda_s R}} \right) \quad (\text{A2})$$

466 where K is the optical wave number (equal to $2\pi/\lambda_s$), C_n^2 is the structure parameter of the refractive
 467 index of air ($\text{m}^{-2/3}$) and f_B describes the decrease of B_{12} with increasing of l_0 (inner length), d_i
 468 (separation between the two sources) and D (diameter of the two detectors) (m). The Eq. (A2)
 469 allows computation of variance of a single beam (B_{11} and B_{22}) simply by assuming $d_i=0$. For given
 470 d_i and D , the ratio $r_{12} = B_{12}/(B_{11}B_{22})^{1/2}$ is a sole function of l_0 , so r_{12} yields directly l_0 . Afterwards,
 471 C_n^2 can be derived from Eq. (A2) for known l_0 and B_{11} (or B_{22}).

472 The so-called ‘‘structure parameter of temperature’’, C_T^2 ($\text{K m}^{-2/3}$), and the ‘‘dissipation rate of the
 473 kinetic energy of the turbulence’’, ε (m^2s^{-3}), can be calculated from C_n^2 and l_0 with:

474
$$C_T^2 = \left(\frac{T_a^2}{b_a P} \right)^2 C_n^2 \quad (\text{A3a})$$

475
$$\varepsilon = \nu^3 \left(\frac{7.4}{l_0} \right)^4 \quad (\text{A3b})$$

476 where b_a is the refractive index coefficient for air at 670 nm, equal to $0.789 \times 10^{-3} \text{ K kPa}^{-1}$, P is
 477 the air pressure (kPa) and ν is the air viscosity ($\text{m}^2 \text{s}^{-1}$).

478 H fluxes are computed from C_T^2 and ε using the Monin-Obukhov Similarity Theory (MOST).
 479 MOST defines H as:

480
$$H = \rho c_p u_* T_* \quad (\text{A4})$$

481 where u_* (m s^{-1}) is the friction velocity and T_* (K) is temperature scale. Both u_* and T_* can be
 482 computed using dimensionless functions. In our experiment the formulation proposed by
 483 Hartogensis (2006) for unstable conditions has been used:

484
$$\varepsilon k z (u_*^{-3}) = \left(1 - 15.1 \frac{z}{L} \right)^{-1/3} - \frac{z}{L} - 0.16 \quad (\text{A5a})$$

485
$$\frac{C_T^2 z^{2/3}}{T_*^2} = 4.9 \left(1 - 6.1 \frac{z}{L} \right)^{-2/3} \quad (\text{A5b})$$

486 and the relationships proposed by Thiermann and Grassl (1992) for stable conditions:

487
$$C_T^2 (0.41z)^{2/3} T_*^2 = 4\beta \left(1 + 7 \frac{z}{L} + 20 \left(\frac{z}{L} \right)^2 \right)^{1/3} \quad (\text{A6a})$$

488 $\varepsilon 0.41z(u_*^{-3}) = \left(1 + 4 \frac{z}{L} + 16 \left(\frac{z}{L} \right)^2 \right)^{-1/2}$ (A6b)

489 where z is the height of the instrument above the zero plane displacement (m), β is the Obukhov-
 490 Corrsin constant (0.86), and L is the Obukhov length (m), equal to:

491 $L = - \frac{\rho c_p T_a u_*^3}{kgH}$ (A7)

492 The relationships (A4)-(A7) allow deriving H fluxes by means of an iterative procedure for both
 493 stable and unstable conditions.

494 The system used in this study case is the optical energy balance measurement system (OEBMS1,
 495 Scintec AG - Germany), which includes a displaced beam small aperture scintillometer (SLS20,
 496 Scintec AG - Germany) to H fluxes, a two component (total incoming and outgoing) pyrradiometer
 497 (model 8111, Schenk GmbH - Germany), and three soil heat plates (HFP01SC, Hukseflux - The
 498 Netherlands).

499 **References**

500 Allen, R.G., Pereira, L.S. 2009. Estimating crop coefficients from fraction of ground cover and
 501 height. *Irrigation Science*. 28(1): 117-34.

502 Allen, R.G., Pereira, L.S., Raes, D., Smith, M., 1998. Crop evapotranspiration. Guideline for
 503 computing crop water requirements. FAO irrigation and drainage paper n. 56, Rome, Italy,
 504 326 pp.

505 Allen, R.G., Pruitt, W.O. 1991. FAO-24 reference evapotranspiration factors. *J. Irrig. Drain. Eng.*
 506 *ASCE*. 117(5):758–773.

507 ASCE-EWRI. 2005. The ASCE standardized reference evapotranspiration equation.
 508 Environmental and Water Resources Institute of the American Society of Civil Engineers
 509 Task Committee on Standardization of reference Evapotranspiration Calculation,
 510 Washington DC, USA, 70 pp.

511 Baldocchi, D., Xu, L. 2007. What limits evaporation from Mediterranean oak woodlands – The
 512 supply of moisture in the soil, physiological control by plants or the demand from
 513 atmosphere? *Adv. Water Resour.* 30, 2113-2122.

514 Blaney, H.F., Criddle, W.D., 1950. Determining Water Requirements in Irrigated Areas from
 515 Climatologically and Irrigation Data. USDA (SCS) TP 96 48.

516 Burke, W., Gabriels, D., Bouma, J., 1986. Soil Structure Assessment. Balkema, Rotterdam, The
517 Netherlands.

518 Cammalleri, C., Ciraolo, G., 2013a. A simple method to directly retrieve reference
519 evapotranspiration from geostationary satellite images. *Int. J. Appl. Earth Obs.* 21, 149-158.

520 Cammalleri, C., Rallo, G., Agnese, C., Ciraolo, G., Minacapilli, M., and Provenzano, G. 2013b.
521 Combined use of eddy covariance and sap flow techniques for partition of ET fluxes and
522 water stress assessment in an irrigated olive orchard. *Agric. Water Manage.*, 120, 89–97.

523 Cammalleri, C., Ciraolo, G., Minacapilli, M., Rallo, G. 2013. Evapotranspiration from an Olive
524 Orchard using Remote Sensing-Based Dual Crop Coefficient Approach *Water Resources
525 Management*, 27 (14), pp. 4877-4895.

526 Castellví, F., Stockle, C.O., Perez, P.J., Ibanez, M. 2001. Comparison of methods for applying
527 Priestley-Taylor equation at a regional scale. *Hydrol. Processes* 15, 1609-1620.

528 de Bruin, H.A.R. 1987. From Penman to Makkink. In J.C. Hooghart (Ed.), *Evaporation and
529 Weather*, (Technical Meeting of the Committee for Hydrological Research, February, 1981),
530 *Comm. Hydrol. Res. TNO, Den Haag, Proc. and Inform.* 39, 5-30.

531 de Bruin, H.A.R., Trigo, I.F., Jitan, M.A., Temesgen Enku, N., van der Tol, C., Gieske, A.S.M.,
532 2010. Reference crop evapotranspiration derived from geo-stationary satellite imagery: a
533 case study for the Fogera flood plain, NW-Ethiopia and the Jordan Valley, Jordan. *Hydrol.
534 Earth Syst. Sci.* 14, 2219-2228.

535 Djaman, K., Balde, A.B., Sow, A., Muller, B., Irmak, S., N'Diaye, M.K., Manneh, B.,
536 Moukoumbi, Y.D., Futakuchi K., Saito, K. 2015. Evaluation of sixteen reference
537 evapotranspiration methods under sahelian conditions in the Senegal River Valley, *Journal
538 of Hydrol., Regional Studies*, 3,139-159, ISSN 2214-5818, doi:10.1016/j.ejrh.2015.02.002.

539 Doorenbos, J., Pruitt, W.O. 1977. Crop water requirements. FAO irrigation and drainage. Paper
540 no. 24 (rev.). FAO, Rome.

541 Hargreaves, G.H., Samani, Z.A., 1985. Reference crop evapotranspiration from temperature. *Appl.
542 Eng. Agric.*, 1 (2), 96-99.

543 Homae, M., Feddes, R., Dirksen, C. 2002. Simulation of root water uptake II. Non-uniform
544 transient water stress using different reduction functions. *Agric. Water. Manage.* 57, 111–
545 126.

546 Jensen, M.E., Haise, H.R. 1963. Estimation of evapotranspiration from solar radiation. *J. Irrig.
547 Drain. Div.* 89, 15–41.

548 Kirkham, M.B. 2014. Principles of soil and plant water relations. Second ed. By M.B. Kirkham.
549 Kansas State University, Throckmorton Plant Science Center, Manhattan. ISBN 978-0-12-
550 420022-7.

551 Kumar, R., Jat, M.K., Shankar, V., 2012. Methods to estimate irrigated reference crop
552 evapotranspiration - A review. *Water Science & Technology*, 66(3):525-35.

553 Liu, B., M. Xu, M. Henderson, and W. Gong, 2004. A spatial analysis of pan evaporation trends
554 in China, 1955–2000, *J. Geophys. Res.*, 109, D15102, doi:10.1029/2004JD004511.

555 Mahringer, W., 1970. Verdunstungsstudien am Neusiedler See. *Theor. Appl. Clim.* 18 (1), 1–20.

556 Makkink, G.F., 1957. Testing the Penman formula by means of lysimeters. *J. Inst. Wat. Engrs.* 11,
557 277-288.

558 Monteith, J.L. 1965. Evaporation and environment. In: G.E. Fogg (Ed.), *The State and Movement*
559 *of Water in Living Organisms*. XIX Sym. Soc. Exp. Biol. 19, 205-234.

560 Penman, H.L. 1948. Natural evaporation from open water, bare soil and grass. *Proceedings of the*
561 *Royal Society of London A*193, 120-146.

562 Pereira, A.R. 2004. The Priestley-Taylor parameter and the decoupling factor for estimating
563 reference evapotranspiration. *Agric. Forest. Meteorol.*, 125, 305-313.

564 Priestley, C.H.B., Taylor, R.J. 1972. On the assessment of surface heat flux and evaporation using
565 large-scale parameters. *Mon. Weather Rev.* 100, 81-92.

566 Provenzano, G., Rallo, G., and Ghazouani, H. (2015). "Assessing Field and Laboratory Calibration
567 Protocols for the Diviner 2000 Probe in a Range of Soils with Different Textures." *J. Irrig.*
568 *Drain Eng.* , 10.1061/(ASCE)IR.1943-4774.0000950 , 04015040.

569 Rallo, G., Provenzano, G. 2015. "Discussion of "Laboratory and Field Calibration of the Diviner
570 2000 Probe in Two Types of Soil" by J. Haberland, R. Gálvez, C. Kremer, and C. Carter." *J.*
571 *Irrig. Drain Eng.*, 141(8), 07014063.

572 Rallo, G., Baiamonte, G., Juárez, J., and Provenzano, G. (2014). "Improvement of FAO-56 Model
573 to Estimate Transpiration Fluxes of Drought Tolerant Crops under Soil Water Deficit:
574 Application for Olive Groves." *J. Irrig. Drain Eng.* 140, SPECIAL ISSUE: Trends and
575 Challenges of Sustainable Irrigated Agriculture, A4014001.

576 Rallo, G., Agnese, C., Minacapilli, M., Provenzano, G. 2012. Comparison of SWAP and FAO
577 Agro-Hydrological Models to Schedule Irrigation of Wine Grapes. *J. Irrig. Drain Eng.*,
578 ASCE, 138(7), 581–591. DOI: 10.1061/(ASCE)IR.1943-4774.0000435.

579 Trabert, W., 1896. Neue Beobachtungen uber " Verdampfungsgeschwindigkeiten. Meteorol. Z.
580 13, 261–263.

581 Thiermann, V., Grassl, H., 1992. The measurement of turbulent surface-layer fluxes by use of
582 bichromatic scintillation. Bound.-Lay. Meteorol. 58, 367–389.

583 Todorovic, M., Kari, B., Pereira L.S. 2013. Reference evapotranspiration estimate with limited
584 weather data across a range of Mediterranean climates. J. of Hydrol., 481, 166–176.

585 Trajković, S., Stojnić, V. 2007. Effect of wind speed on accuracy of Turc method in a humid
586 climate. Facta Universitatis, Series: Arch. Civil Eng., 5(2), 107-113.

587 Turc, L. 1961. Estimation of irrigation water requirements, potential evapotranspiration: a simple
588 climatic formula evolved up to date. Annals of Agron., 12, 13-49.

589 Valiantzas, J. 2013. Simplified forms for the standardized FAO-56 Penman–Monteith reference
590 evapotranspiration using limited weather data. J. of Hydrol., 505: 13-23.

591 Valipour, M. 2014a. Analysis of potential evapotranspiration using limited weather data. Applied
592 Water Scie., ISSN 2190-5487. DOI 10.1007/s13201-014-0234-2.

593 Valipour, M. 2014b. Comparative Evaluation of Radiation-Based Methods for Estimation of
594 Potential Evapotranspiration. J. of Hydrol. Eng., ASCE, ISSN 1084-0699/04014068(14).

595 Valipour, M. 2014c. Use of average data of 181 synoptic stations for estimation of reference crop
596 evapotranspiration by temperature-based methods. Water Resources Management. Vol.
597 28(12), 4237-4255.

598 Valipour, M., Eslamian S. 2014. Analysis of potential evapotranspiration using 11 modified
599 temperature-based models. International Journal of Hydrology Science and Technology
600 (IJHST), Vol. 4(3).

601 Valipour, M. 2015a. Investigation of Valiantzas' evapotranspiration equation in Iran. Theoretical
602 and Applied Climatology. Vol. 121(1), 267-278.

603 Valipour, M. 2015b. Importance of solar radiation, temperature, relative humidity, and wind speed
604 for calculation of reference evapotranspiration. Archives of Agronomy and Soil Science.
605 Vol. 61(2), 239-255.

606 Valipour, M. 2015c. Evaluation of radiation methods to study potential evapotranspiration of 31
607 provinces. Meteorology and Atmospheric Physics, Vol. 127(3), 289-303.

608 Valipour, M. 2015d. Study of different climatic conditions to assess the role of solar radiation in
609 reference crop evapotranspiration equations. Archives of Agronomy and Soil Science.
610 Vol.61(5), 679-694.

611 Valipour, M. 2015e. Estimation of actual evapotranspiration by using MODIS images (a case
612 study: Tajan catchment). Archives of Agronomy and Soil Science. Vol.61(5), 695-709.

613 Valipour, M. 2015f, Temperature analysis of reference evapotranspiration models. Met. Apps, 22:
614 385–394. doi: 10.1002/met.1465.

615 van Genuchten, M.T. 1980. A closed form equation for predicting the hydraulic conductivity of
616 unsaturated soils. Soil Science Society of America Journal. 44, 892–898.

617 van Genuchten, M.T., Leij, F.J., Yates, S.R., 1992. The RETC code for quantifying the hydraulic
618 functions of unsaturated soils. Project summary, EPA’S Robert S. Kerr Environmental
619 Research Lab., Ada, OK, USA.

620 Villalobos, F.J., Mateos, L., Orgaz, F., Fereres, E. 2002. Fitotecnia. Bases y tecnología de la
621 producción agrícola. Mundi-Prensa, Madrid, Spain.

622 WMO. 1966. Measurement and estimation of evaporation and evapotranspiration. Tech Pap.
623 (CIMO-Rep) 83. Genf.

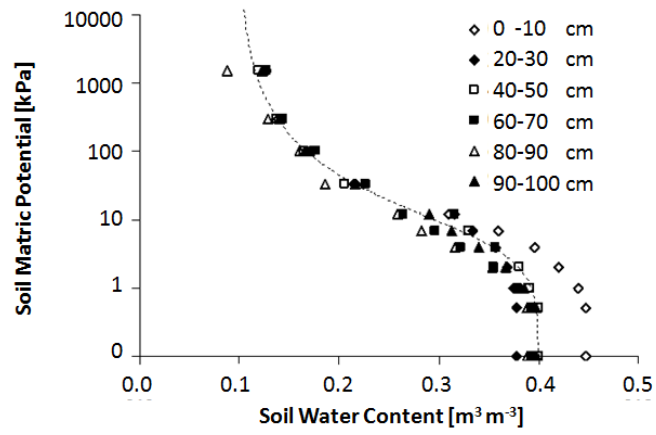
624

625

626

Figures and Tables

627

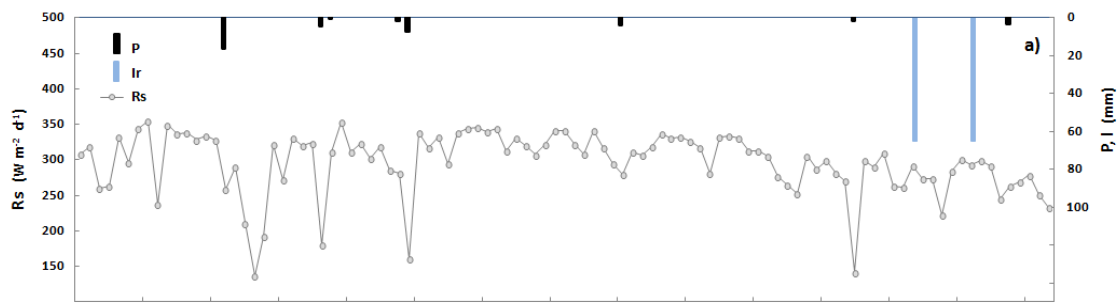


628

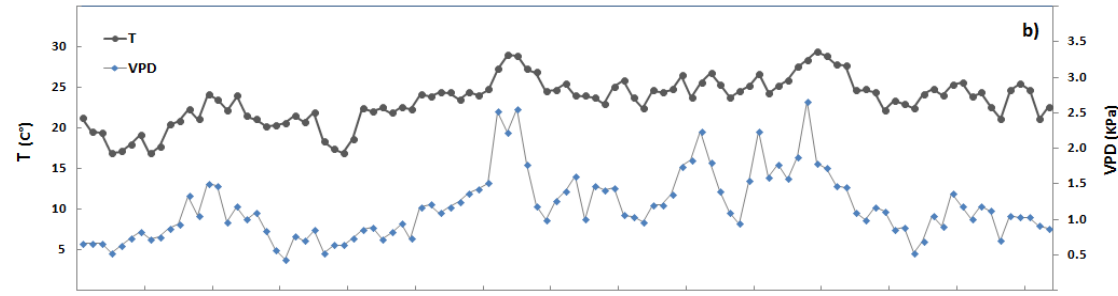
629 Fig. 1 - Soil water retention data obtained at the different depths. Dotted line
630 represents the van Genuchten fitting model

631

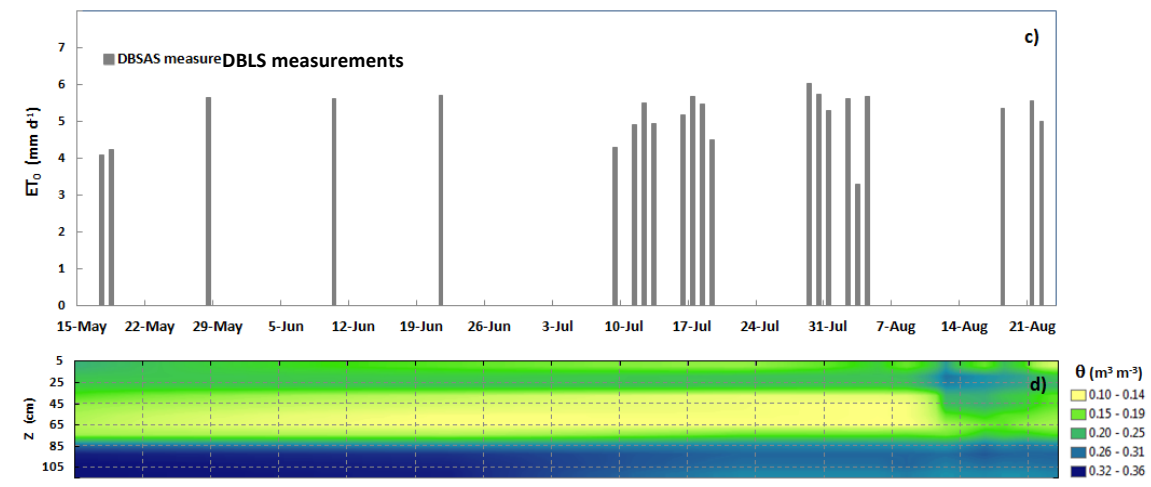
632



633



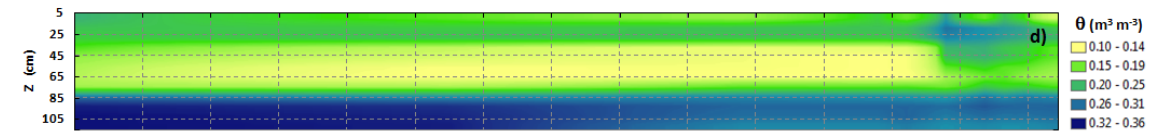
634



635

Fig. 2 a,d – Main variables measured at daily scale: a) Shortwave radiation, R_s , Precipitation, P and Irrigation, I ; b) Mean air temperature, T and Vapor Pressure Deficit, VPD ; c) Observed Evapotranspiration (DBLS scintillometer), ET_0 ; d) Dynamic of Soil water content, **SWC**

639



640

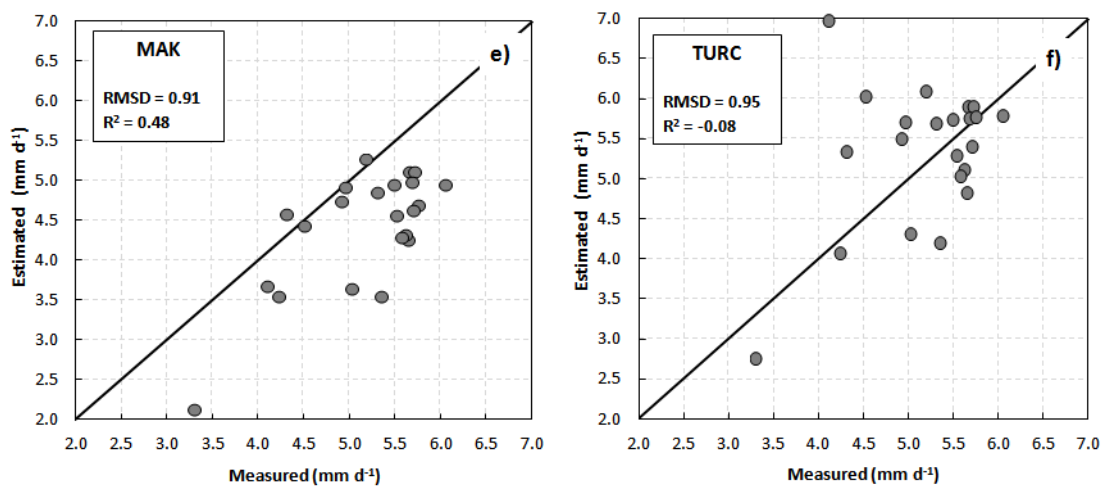
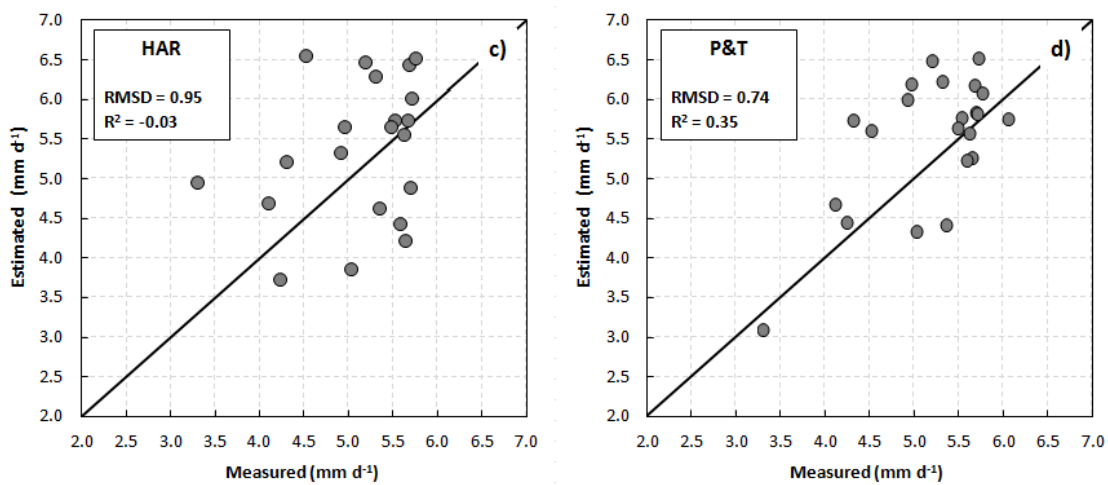
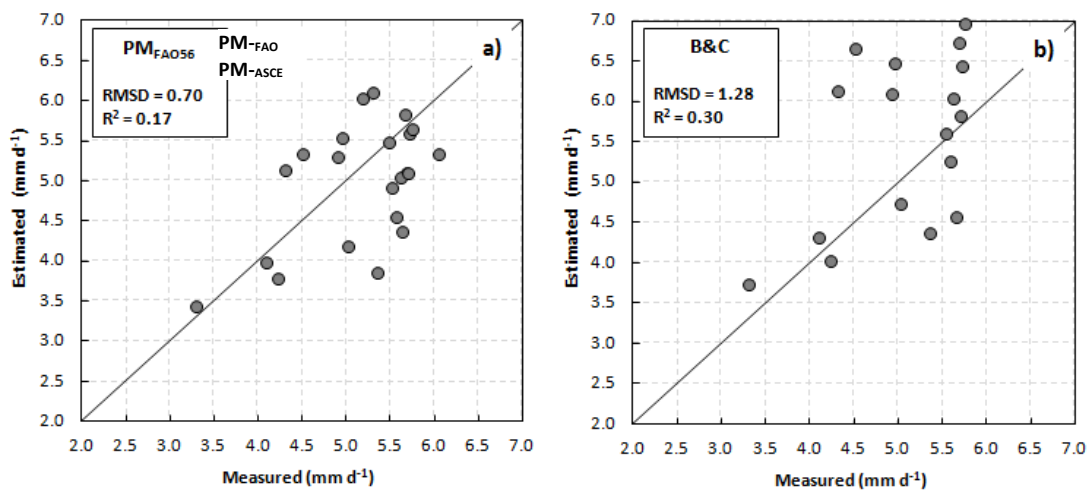
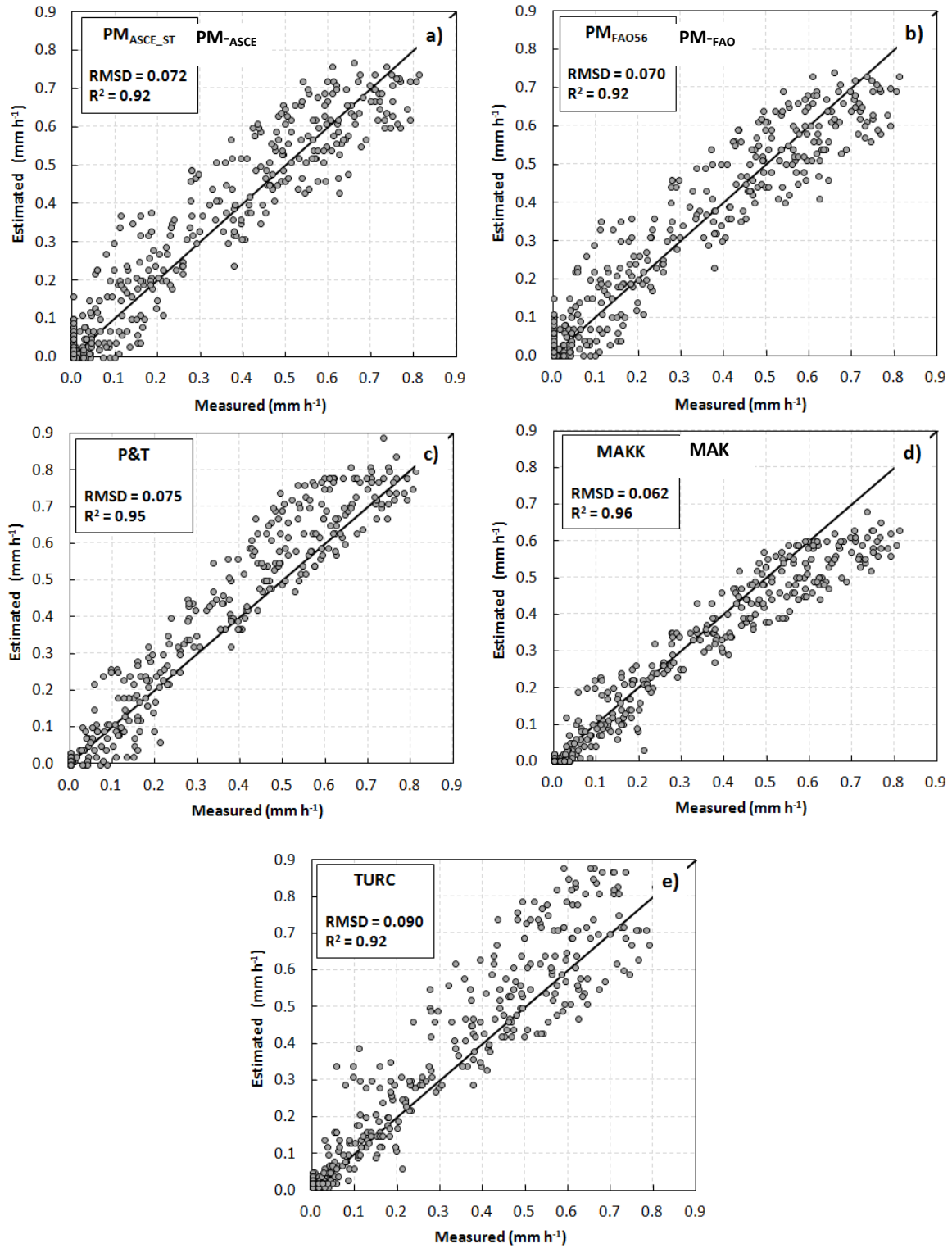


Fig. 3 – Measured vs. predicted daily evapotranspiration



646

647

648

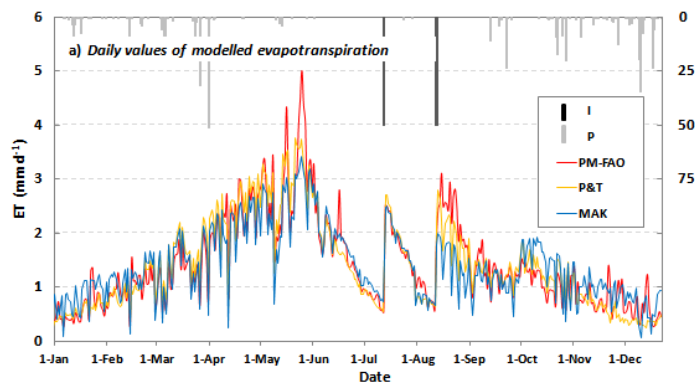
649

650

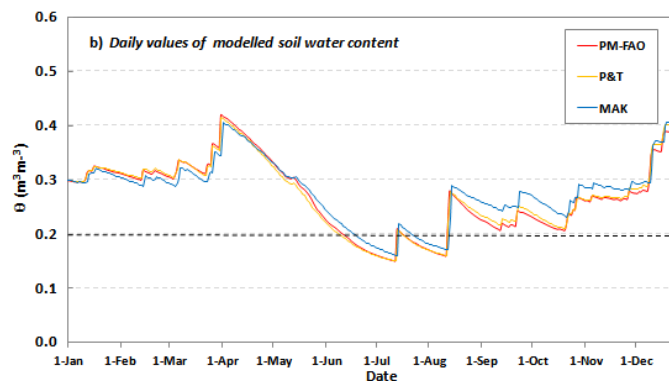
651

Fig. 4 – Measured vs. predicted hourly evapotranspiration

652



653



654

655

656

Fig. 5 – Dynamic of daily **and** actual evapotranspiration and soil water content obtained for olive groves by using the different methods to estimate ET_0

657

658

659

660

661

662

663

664

665

666

667

668

669

670

671

672

Table 1. Meteorological variables required by the different ET_0 computation methods

673

Method	Acronym	Time-step	R_s	T_a	RH	u
Penman-Monteith FAO56	PM-FAO	hourly/daily	×	×	×	×
Penman-Monteith ASCE	PM-ASCE	hourly/daily	×	×	×	×
Pristely & Taylor	P&T	hourly/daily	×	×	×	
Makkink	MAK	hourly/daily	×	×		
Turc	TURC	hourly/daily	×	×		
Blaney-Criddle	B&C	Daily	×	×	×	
Hargreaves	HAR	Daily		×		

674

675

676

677

678 Table 2 – Statistical indicators computed by comparing daily evapotranspiration
 679 obtained with the different methods (dependent variable) and observations
 680 (independent variable)
 681

Methods	MAD (mm d ⁻¹)	RMSD (mm d ⁻¹)	Slope (-)	R² (-)	RE %	MBE (mm d ⁻¹)	T (-)
PM-FAO/PM-ASCE	0.59	0.70	1.0	0.17	11.45	-0.15	0.355
P&T	0.60	0.74	1.1	0.35	11.60	0.35	0.023
MAK	0.77	0.91	0.9	0.48	14.89	-0.73	0.000
TURC	0.66	0.95	1.0	-0.08	12.78	0.20	0.327
B&C	1.06	1.28	1.2	0.30	20.54	0.80	0.001
HAR	0.81	0.95	1.0	-0.03	15.70	0.29	0.162

682

683

684

685 Table 3 – Statistical indicators computed by comparing hourly and daily
 686 evapotranspiration obtained with the different methods (dependent variable) and
 687 observations (independent variable). Daily ET₀ estimations are evaluated by
 688 integrating hourly data
 689

Methods	MAD		RMSD		Slope		R ²		RE		MBE		T	
	<i>Hourly</i>	<i>Daily</i>	<i>Hourly</i>	<i>Daily</i>	<i>Hourly</i>	<i>Daily</i>	<i>Hourly</i>	<i>Daily</i>	<i>Hourly</i>	<i>Daily</i>	<i>Hourly</i>	<i>Daily</i>	<i>Hourly</i>	<i>Daily</i>
	(mm h ⁻¹)	(mm d ⁻¹)	(mm h ⁻¹)	(mm d ⁻¹)	(-)	(-)	(mm h ⁻¹)	(mm d ⁻¹)	(-)	(-)	%	%	(-)	(-)
PM-ASCE	0.05	0.61	0.07	0.73	1.0	1.0	0.01	0.27	0.92	0.24	23.98	11.86	0.004	0.066
PM-FAO	0.05	0.58	0.07	0.67	1.0	1.0	0.00	0.06	0.92	0.28	23.57	11.24	0.402	0.086
P&T	0.05	0.63	0.07	0.78	1.1	1.1	0.02	0.43	0.95	0.42	24.65	12.30	0.000	0.006
MAK	0.04	0.65	0.06	0.79	0.9	0.9	-0.02	-0.59	0.96	0.49	18.02	12.65	0.000	0.000
TURC	0.06	1.13	0.09	1.38	1.1	1.2	0.04	0.98	0.92	0.46	27.10	21.99	0.000	0.000

690

691

692